NEUROSCIENCE
RESEARCH ARTICLE
G. Terral et al. / Neuroscience 433 (2020) 121–131

Synaptic Functions of Type-1 Cannabinoid Receptors in Inhibitory Circuits of the Anterior Piriform Cortex

Geoffrey Terral, [a,b] **Marjorie Varilh,** [a,b] **Astrid Cannich,** [a,b] **Federico Massa,** [a,b] **Guillaume Ferreira** [b,c†] **and Giovanni Marsicano** [a,b*†]

[a] *INSERM, U1215 NeuroCentre Magendie, 146 rue Léo Saignat, 33077 Bordeaux Cedex, France*

[b] *University of Bordeaux, 146 rue Léo Saignat, 33000 Bordeaux, France*

[c] *INRAE, Bordeaux INP, Nutrition and Integrative Neurobiology, UMR 1286, 146 rue Léo Saignat, 33076 Bordeaux Cedex, France*

Abstract—In the olfactory system, the endocannabinoid system (ECS) regulates sensory perception and memory. A major structure involved in these processes is the anterior piriform cortex (aPC), but the impact of ECS signaling in aPC circuitry is still scantly characterized. Using *ex vivo* patch clamp experiments in mice and neuroanatomical approaches, we show that the two major forms of ECS-dependent synaptic plasticity, namely depolarization-dependent suppression of inhibition (DSI) and long-term depression of inhibitory transmission (iLTD) are present in the aPC. Interestingly, iLTD expression depends on layer localization of the inhibitory neurons associated with the expression of the neuropeptide cholecystokinin. Conversely, the decrease of inhibitory transmission induced by exogenous cannabinoid agonists or DSI do not seem to be impacted by these factors. Altogether, these results indicate that CB1 receptors exert an anatomically specific and differential control of inhibitory plasticity in the aPC, likely involved in spatiotemporal regulation of olfactory processes.

Key words: CB1 receptors, anterior piriform cortex, DSI, iLTD, mice.

INTRODUCTION

Neuromodulators play crucial roles in shaping neuronal functions in the brain. The regulation of synaptic transmission is provided by a variety of neuromodulatory systems (Nadim and Bucher, 2014; Avery and Krichmar, 2017). G protein-coupled receptors (GPCRs) are the principal effectors of most of these synaptic modulatory activities (Betke et al., 2012; Huang and Thathiah, 2015). Cannabinoid type-1 (CB1) receptors have been characterized as the most abundant GPCRs in the brain (Herkenham et al., 1990; Howlett et al., 2002) and they are expressed in various cell types—glutamatergic and GABAergic neurons as well as glial cells—and in different cellular compartments (Marsicano and Kuner, 2008; Kano et al., 2009; Bénard et al., 2012; Araque et al., 2017; Busquets-Garcia et al., 2018a; Zou and Kumar, 2018). Together with their endogenous lipid ligands (endocannabinoids) and the enzymatic machineries responsible for endocannabinoid synthesis and degradation, CB1 receptors are the main components of the endocannabinoid system (ECS) in the brain (Piomelli, 2003; Piazza et al., 2017). In neurons, activation of presynaptic CB1 receptors results in the decrease of neurotransmitter release, inducing several forms of ECS-dependent synaptic plasticity (Kano et al., 2009; Castillo et al., 2012; Araque et al., 2017; Busquets-Garcia et al., 2018a; Zou and Kumar, 2018). In many brain regions, expression of CB1 receptors in specific subpopulations of GABAergic interneurons mediates short- and long-term forms of ECS-dependent plasticity of inhibitory neurotransmission, such as depolarization-induced suppression of inhibition (DSI) (Wilson and Nicoll, 2001) and inhibitory long-term depression (iLTD) (Marsicano et al., 2002; Chevaleyre and Castillo, 2003).

Given the wide expression of CB1 receptors in multiple brain areas, including cortical and subcortical ones (Marsicano and Kuner, 2008), the ECS modulates a large variety of cognitive processes (Kano et al.,

*Correspondence to: G. Marsicano, 146 rue Léo Saignat, 33077 Bordeaux Cedex, France.
E-mail address: giovanni.marsicano@inserm.fr (G. Marsicano).

† These authors share senior authorship.

Abbreviations: aPC, anterior piriform cortex; CB1, cannabinoid type-1; CCK, cholecystokinin; DAPI, 4′,6-diamidino-2-phenylindole; DSI, depolarization-induced suppression of inhibition; ECS, endocannabinoid system; EGTA, ethylene glycol-bis(β-aminoethyl ether)-N,N,N′,N′-tetraacetic acid; eIPSCs, evoked inhibitory post-synaptic currents; FISH, Fluorescent *in situ* hybridization; GPCRs, G protein-coupled receptors; HEPES, 4-(2-hydroxyethyl)-1-piperazineethanesulfonic acid; HFS, High-Frequency-Stimulation; HRP, horseradish peroxidase; iLTD, inhibitory Long-Term Depression; mGluRs, metabotropic glutamate receptors; PBS, phosphate-buffered solution; TSA, tyramide signal amplification.

https://doi.org/10.1016/j.neuroscience.2020.03.002
0306-4522/

2009; Araque et al., 2017; Busquets-Garcia et al., 2018a). For example, CB1 receptors control olfactory-related behaviors by regulating glutamatergic neurotransmission in the olfactory bulb (Soria-Gómez et al., 2014) and GABAergic signaling in the anterior piriform cortex (aPC; Terral et al., 2019). The aPC consists of three layers all harboring several types of interneurons (Suzuki and Bekkers, 2007, 2010a, 2010b, 2012), which have been proposed to play crucial roles in shaping olfactory processes (Poo and Isaacson, 2009; Zhan and Luo, 2010; Franks et al., 2011; Suzuki and Bekkers, 2012; Bolding and Franks, 2018).

Recently, the regulation of neurotransmission and plasticity by CB1 receptors in the olfactory bulb has been the center of large attention (Wang et al., 2012, 2019; Soria-Gómez et al., 2014; Pouille and Schoppa, 2018). However, little is known about the synaptic neuromodulation exerted by CB1 receptors in higher olfactory structures, such as the aPC (Terral et al., 2019). ECS-dependent plasticity and pharmacological effects of cannabinoid ligands on synaptic transmission have been widely investigated in the hippocampus, where anatomical and functional constraints were observed to regulate these phenomena. However, nothing is currently known if analogous properties exist in cortical olfactory structures such as the aPC.

In this study, we characterized the pharmacological and physiological impact of (endo)cannabinoid signaling on the regulation of inhibitory synapses in the aPC. The results show that the anatomical distribution and the neurochemical features of local interneurons expressing CB1 receptors is linked to a differential regulation of synaptic functions by ECS. Whereas DSI and the inhibitory effect of exogenous agonists are present when inhibitory fibers from all layers are stimulated, iLTD is restricted to inhibitory synapses activated in layers II and III. Interestingly, local interneurons containing CB1 receptors in layer I lack cholecystokinin (CCK) expression, which is present in the other layers, suggesting that this neurochemical feature is necessary for long-term control of synaptic plasticity by the ECS.

EXPERIMENTAL PROCEDURES

Animals

All experimental procedures were approved by the local Committee on Animal Health and Care of Bordeaux (authorization number A33063098). Animals were housed under a 12–12 h light–dark cycle with food and water ad libitum. 8 to 12 weeks male CB1-flox mice (mice carrying the "floxed" CB1 gene *Cnr1*) were used (Marsicano et al., 2002, 2003; Monory et al., 2006). Conditional knockout mice lacking CB1 receptors in forebrain GABAergic Dlx5/6 positive neurons (GABA-*CB1*-KO) were obtained as described before (Monory et al., 2006; Bellocchio et al., 2010). Briefly, Dlx5/6-Cre mice were crossed with CB1-flox mice, allowing the deletion of CB1 receptors specifically in GABAergic neurons, named as GABA-*CB1*-KO mouse line.

Ex vivo electrophysiology

Brain slices were taken from the aPC as previously described (Terral et al., 2019). Slices were continuously oxygenated with 95% O2/5% CO2 in ACSF containing in mM: 123 NaCl, 26 $NaHCO_3$, 11 Glucose, 2.5 KCL, 2.5 CaCl2, 1.3 $MgCl_2$, 1.25 NaH_2PO_4 (Sigma) ≈ 305 mOsm at 32 °C during recordings. Whole-cell patch clamp experiments were performed in semilunar neurons, identified by their location, morphology and electrical properties (Suzuki and Bekkers, 2006, 2011; Terral et al., 2019). These neurons were clamped at −70 mV (Molecular Devices, UK) with glass pipettes (3–5 MΩ). Evoked inhibitory post-synaptic currents (eIPSCs) were recorded with an internal solution containing in mM: 130 KCl, 10 HEPES, 1 EGTA, 2 $MgCl_2$, 0.3 CaCl2, 7 Phosphocreatin, 3 Mg-ATP, 0.3Na-GTP (Sigma); pH = 7.2; 290 mOsm, in presence of NMDA and AMPA/Kainate receptor antagonists (50 μM D-APV and 10 μM NBQX, Abcam). Monopolar stimulating patch pipettes filled with ACSF were placed in layer Ib, II or III to evoked inhibitory post-synaptic currents (layer I, layer II and layer III eIPSCs).

For WIN 55212-2 (WIN) experiments, eIPSCs were obtained every 20 s using paired stimulation with 175 ms apart and the ratio between the mean amplitudes of the second eIPSC over the first eIPSC (paired-pulse ratio, PPR) was measured. The effect of WIN was assessed by comparing the mean of the 10 min baseline with the average responses between 20 and 25 min after drug application.

DSI experiments were performed by evoking IPSCs every 3 s and depolarizing semilunar neurons from −70 mV to 0 mV for 5 s. DSI magnitude was measured as the average of three trials with 2 min apart and represented as the percentage of change by comparing the first three eIPSCs following the depolarization with the five consecutives eIPSCs preceding the depolarization.

Only cells in which DSI was obtain (only one trial to evaluate the presence of DSI) were used for iLTD experiments. iLTD was induced by evoking IPSCs every 20 s and two trains of High-Frequency-Stimulation (HFS) of 100 pulses at 100 Hz were delivered with 20 s apart after a minimum of 10 min of stable baseline. iLTD magnitude was represented by the percentage of change between the mean of the 10 min baseline with the percentage of responses averaged between 20 and 25 min after HFS.

WIN (5 μM; Sigma) and AM251 (4 μM; Tocris Bioscience) were prepared in DMSO (Sigma) and applied in the slices a minimum 15 min prior DSI or iLTD experiments.

Signals were filtered at 4 kHz by a Digidata 1440A (Molecular Devices, UK) and analyzed using Clampfit software (pClamp10).

Fluorescent *in situ* hybridization

The procedure was adapted from previous studies (Marsicano and Lutz, 1999; Soria-Gómez et al., 2014; Terral et al., 2019). Mice were anesthetized with pentobarbital (Exagon, 400 mg/kg body weigh), transcardially

perfused with phosphate-buffered solution (PBS 0.1 M, pH 7.4) before being fixed with 4% paraformaldehyde and quickly frozen by immersion in isopentane then stored at −80 °C. Serial coronal free-floating sections were cut at 30 μm in a cryostat (Microm HM 500 M, Microm Microtech). Fluorescein (FITC)-labeled riboprobes against mouse CB1 receptor and Digoxigenin (DIG)-labeled riboprobes against mouse GAD65/67 and CCK were prepared as described (Marsicano and Lutz, 1999). The slices were incubated with the hybridization buffer containing the mixture of probes overnight at 62 °C. After hybridization, the sections were washed with different stringency wash buffers at 67 °C and blocked with a blocking buffer prepared according to the manufacturer's protocol. Anti-FITC or anti-DIG antibodies conjugated to horseradish peroxidase (HRP) (Roche; 1:2000) were applied 2 h at room temperature or overnight at 4 °C to detect respectively CB1-FITC or GAD65/67-DIG and CCK-DIG probes. Probes hybridization was revealed by a tyramide signal amplification (TSA) reaction using FITC-labeled tyramide (Perkin Elmer; 1:80 for 12 min) to detect CB1 signal or Cyanine 3-conjugated tyramide (Perkin Elmer; 1:100 for 10 min) to amplify the signal of GAD65/67 or CCK. The slices were incubated in 4′,6-diamidino-2-phenylindole (DAPI; 1:20,000; FISHER Scientific, NH, USA) before being washed, mounted, coverslipped and visualized with an epifluorescence Leica DM6000 microscope (Leica, Germany).

Quantitative co-expression data were obtained using ImageJ, by counting CB1 (green) and GAD65/67 or CCK (red) and co-expressing neurons. According to the different level of CB1-expressing cells, High- and Low-CB1 cells were distinguished as previously defined (Marsicano and Lutz, 1999; Terral et al., 2019). The numerical evaluation was performed at X10 magnification in 20 sections from three different mice.

Statistical analysis

Data were analyzed with Prism Software (GraphPad). For each group difference from baseline was analyzed using one sample Student's *t*-test. Comparisons between groups were obtained with unpaired Student's *t*-test or one-way ANOVA. When ANOVA provided significant main factor effects or significant interactions, Tukey or Dunnett post-hoc analyses were performed as appropriate. Types of statistical tests are presented in figure legends. Significance was set at $p < 0.05$ and data are expressed as mean ± SEM and represented as mean ± SEM or median ± quartiles in Figures. For statistical details, see Table1.

RESULTS

Exogenous activation of CB1 receptors reduces evoked inhibitory transmission in the aPC

We have previously shown that the CB1 receptor agonist WIN 55212-2 (WIN) decreases the frequency of miniature inhibitory post-synaptic currents in principal cells of the aPC (Terral et al., 2019). However, this method does not allow evaluating the anatomical distribution of inhibitory inputs depressed by CB1 receptor activation. Thus, we tested the impact of WIN on evoked inhibitory post-synaptic currents (eIPSCs) recorded in principal neurons, by placing the stimulating electrode in the different layers of the aPC, to generate "layer I, layer II and layer III eIPSCs", respectively (see methods, Fig. 1A). We found that WIN application induced a significant reduction of eIPSCs as compared to baseline in all layers (layer I, −64.1 ± 4.5%; layer II, −42.4 ± 5.4%; layer III, −61.1 ± 6.4%; Fig. 1B, C). Interestingly, the effect of WIN was stronger in layer I and layer III than in layer II (Fig. 1B, C). Supporting a presynaptic mechanism of action, these effects were accompanied by a significant increase of the paired-pulse ratio as compared to baseline (PPR; layer I, 54.2 ± 18.7%; layer II, 33.8 ± 12.8%; layer III, 110 ± 15.7%; Fig. 1D), which was stronger in layer III than in the other layers (Fig. 1D). In contrast, the agonist was not able to affect evoked layer III IPSCs amplitude (0.4 ± 6 %; Fig. 1B, C) nor the PPR (1.6 ± 7%; Fig. 1D) in conditional mutant mice carrying a specific deletion of the *CB1* receptor gene in forebrain GABAergic cells (GABA-*CB1*-KO mice) (Monory et al., 2006; Bellocchio et al., 2010). These results indicate that pharmacological activation of CB1 receptors in GABAergic interneurons of all layers reduces evoked inhibitory synaptic transmission onto principal cells of the aPC. Interestingly, the intensity of this effect and the associated changes in PPR appear to be modulated by the anatomical location of the interneurons involved.

DSI is present in all three layers of aPC

Endocannabinoid signaling mediates several forms of plasticity of inhibitory transmission, which are best characterized in the hippocampus (Kano et al., 2009; Castillo et al., 2012; Araque et al., 2017). Depolarization-induced suppression of inhibition (DSI) is a classic form of ECS-dependent retrograde short-term synaptic plasticity induced by depolarization steps of the postsynaptic neuron eventually triggering activation of presynaptic CB1 receptors (Wilson and Nicoll, 2001; Kano et al., 2009; Castillo et al., 2012; Araque et al., 2017). Independently of the stimulation site, transient depolarization (5 s from −70 mV to 0 mV) of the postsynaptic principal cells induced reliable DSI in the aPC, which consisted in an approximate 30% reduction of eIPSCs amplitudes (Fig. 2A-C). Next, we assessed whether aPC DSI depends on activation of CB1 receptors. A specific feature defining ECS-dependent DSI is that its expression is blocked or occluded by application of CB1 receptor antagonists or agonists, respectively (Wilson and Nicoll, 2001; Kano et al., 2009). Importantly, the CB1 receptor antagonist AM251 (4 μM) significantly blunted DSI in all layers (layer I, from −30.6 ± 2.1% to −12.2 ± 4.6%; layer II, from −27.3 ± 2.6% to −2.3 ± 3.7%; layer III, from −26 ± 2.9% to −4.5 ± 3.4%; Fig. 2C). Similarly, the application of the CB1 receptor agonist WIN (5 μM) occluded DSI in both layers (layer I, 1.24 ± 3.5%; layer III, −1.22 ± 2.8%; Fig. 2C). Moreover, DSI was also blunted in GABA-*CB1*-KO mice after stimulation of layer I or III (layer I: −11.8 ± 3.5%; layer III: 1.79 ± 8.5%; Fig. 2C). Altogether, these results indi-

Table 1.

Figure	Variable	Mean	SEM	*n*	Statistical test – main *P* values			Post hoc analysis – *P* values
1C	Layer I	−64.1	4.5	11	*One sample t-test*		*One-way ANOVA*	*Tukey*
					$t = 14.2$; df = 10		$F(3,33) = 37.2$	Layer I vs Layer II
					$p < 0.0001$		$p < 0.0001$	$p = 0.007$
	Layer II	−42.4	5.4	8	$t = 10.9$; df = 7			Layer I vs Layer III
					$p < 0.0001$			$p = 0.96$
	Layer III	−61.1	6.4	12	$t = 9.5$; df = 11			Layer II vs Layer III
					$p < 0.0001$			$p = 0.002$
	GABA-*CB1*-KO	0.4	6	6	$t = 0.06$; df = 5			
					$p = 0.96$			
1D	Layer I	54.2	18.7	11	*One sample t-test*		*One-way ANOVA*	*Tukey*
					$t = 2.9$; df = 10		$F(3,33) = 7.9$	Layer I vs Layer II
					$p = 0.02$		$p = 0.0005$	$p = 0.82$
	Layer II	33.8	12.8	8	$t = 2.6$; df = 7			Layer I vs Layer III
					$p = 0.04$			$p = 0.051$
	Layer III	110	15.7	12	$t = 7.0$; df = 11			Layer II vs Layer III
					$p < 0.0001$			$p = 0.011$
	GABA-*CB1*-KO	1.6	7	6	$t = 0.2$; df = 5			
					$p = 0.83$			
2C	Layer I, Control	−30.6	2.1	40	*One-way ANOVA*			*Dunnett*
	Layer I, AM251	−12.3	4.6	10	$F(3,74) = 17.9$			Control vs AM251
	Layer I, WIN	1.2	3.6	8	$p < 0.0001$			$p = 0.0009$
	Layer I, GABA-*CB1*-KO	−11.8	3.5	20				Control vs WIN
								$p < 0.0001$
								Control vs GABA-*CB1*-KO
								$p < 0.0001$
	Layer II, Control	−27.3	2.6	31	*Unpaired t-test*			
	Layer II, AM251	−2.3	3.7	16	$t = 5.5$; df = 45			
					$p < 0.0001$			
	Layer III, Control	−26	2.9	22	*One-way ANOVA*			*Dunnett*
	Layer IIII, AM251	−4.5	3.4	10	$F(3,43) = 14.1$			Control vs AM251
	Layer IIII, WIN	−1.2	2.8	10	$p < 0.0001$			$p = 0.0002$
	Layer IIII, GABA-*CB1*-KO	1.8	8.5	5				Control vs WIN
								$p < 0.0001$
								Control vs GABA-*CB1*-KO
								$p = 0.0002$
3D	Layer I, Control	14.9	7.9	5	*One sample t-test*		*One-way ANOVA*	*Tukey*
					$t = 1.9$; df = 4		$F(4,29) = 4.6$	Layer I vs Layer II
					$p = 0.13$		$p = 0.006$	$p = 0.03$
	Layer II, Control	−41.5	12.6	6	$t = 3.3$; df = 5	*Unpaired t-test*		Layer I vs Layer III
					$p = 0.02$	$t = 3.06$;		$p = 0.045$
	Layer II, AM251	0.13	5.3	6	$t = 0.02$;	df = 10		Layer II vs Layer III
					df = 5	$p = 0.012$		$p = 0.99$
					$p = 0.98$			
	Layer III, Control	−34.7	12.2	8	$t = 2.8$; df = 7	*Unpaired t-test*		
					$p = 0.03$	$t = 2.22$;		
	Layer III, AM251	3.1	11.8	9	$t = 0.3$; df = 8	df = 15		
					$p = 0.80$	$p = 0.04$		

cate that aPC DSI is a *bona fide* CB1 receptor-dependent form of synaptic plasticity that is due to the endogenous activation of CB1 receptors at GABAergic terminals impinging onto principal neurons. Thus, CB1 receptor-dependent pharmacological reduction of eIPSCs and DSI are present in all layers of aPC.

The expression of iLTD is limited to layers II and III of aPC

Whereas short post-synaptic depolarization induces transient short-term DSI, repeated high frequency stimulation (HFS) of afferent fibers results in a long-term form of ECS-dependent synaptic plasticity of eIPSCs in the hippocampus and other brain regions, generally called inhibitory long-term depression (iLTD) (Chevaleyre and Castillo, 2003; Crosby et al., 2011). Thus, we applied two HFS trains to afferent fibers in layer I, II or III, respectively, while recording eIPSCs in layer II principal neurons. As described in the hippocampus (Chevaleyre and Castillo, 2004; Younts et al., 2016), only cells displaying reliable DSI were used for these experiments (see methods). However, HFS surprisingly failed to produce a significant long-term decrease of eIPSCs

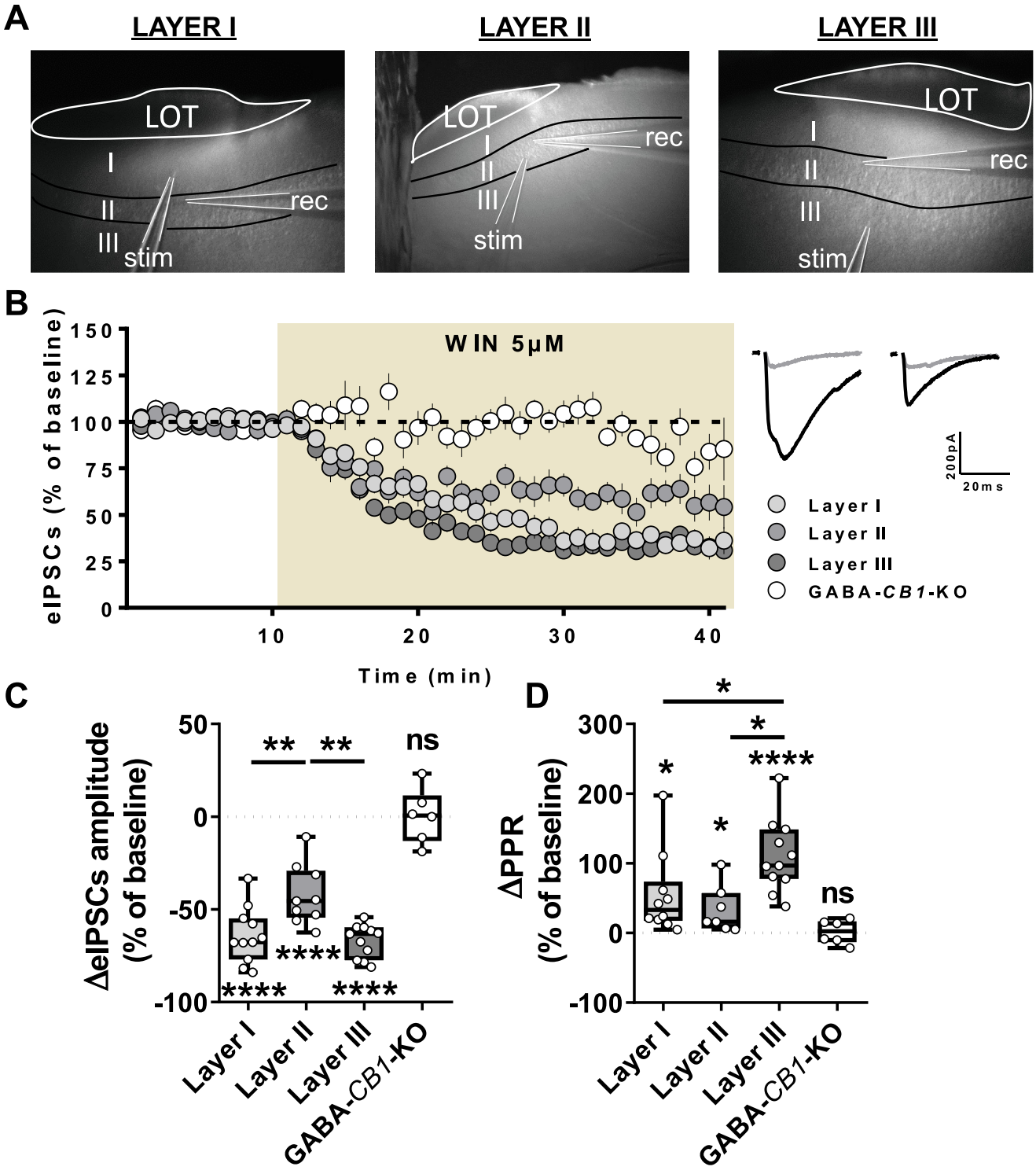

Fig. 1. **(A)** Representative images showing the position of the stimulating electrodes in the different layers while recording evoked inhibitory post-synaptic currents (eIPSCs) in principal neurons of the aPC, producing ''layer I, layer II and layer III eIPSCs". **(B, D)** Effect of the CB1 receptor agonist WIN 55212-2 (5 μM) on eIPSCs in the different layers of wild-type or in layer III of GABA-*CB1*-KO mice. **(B)** Left, average time course of eIPSCs recorded before and after WIN application. Right, representative eIPSC paired stimulation traces before (black) and after (grey) WIN application. **(C)** Percentage reduction of eIPSCs and **(D)** PPR after WIN application. Layer I (n = 11), Layer II (n = 9), Layer III (n = 12), GABA-*CB1*-KO (Layer III, n = 6). One sample t-test and one-way ANOVA ($p < 0.001$), Tukey post hoc. ****$p < 0.0001$; **$p < 0.01$; *$p < 0.05$; ns, not significant. Values are represented mean ± SEM (**B**) and median ± quartiles (**C,D**). For statistical details, see Table 1.

when the stimulation was applied to layer I (14.9 ± 7.9%; Fig. 3A, D). Conversely, significant iLTD was obtained when the stimulating electrodes were placed either in layer II (−41.5 ± 12.6%; Fig. 3B, D) or in layer III (−34.7 ± 12.2% SEM; Fig. 3C, D). Importantly, iLTD was blocked by the application of AM251 in both layer II

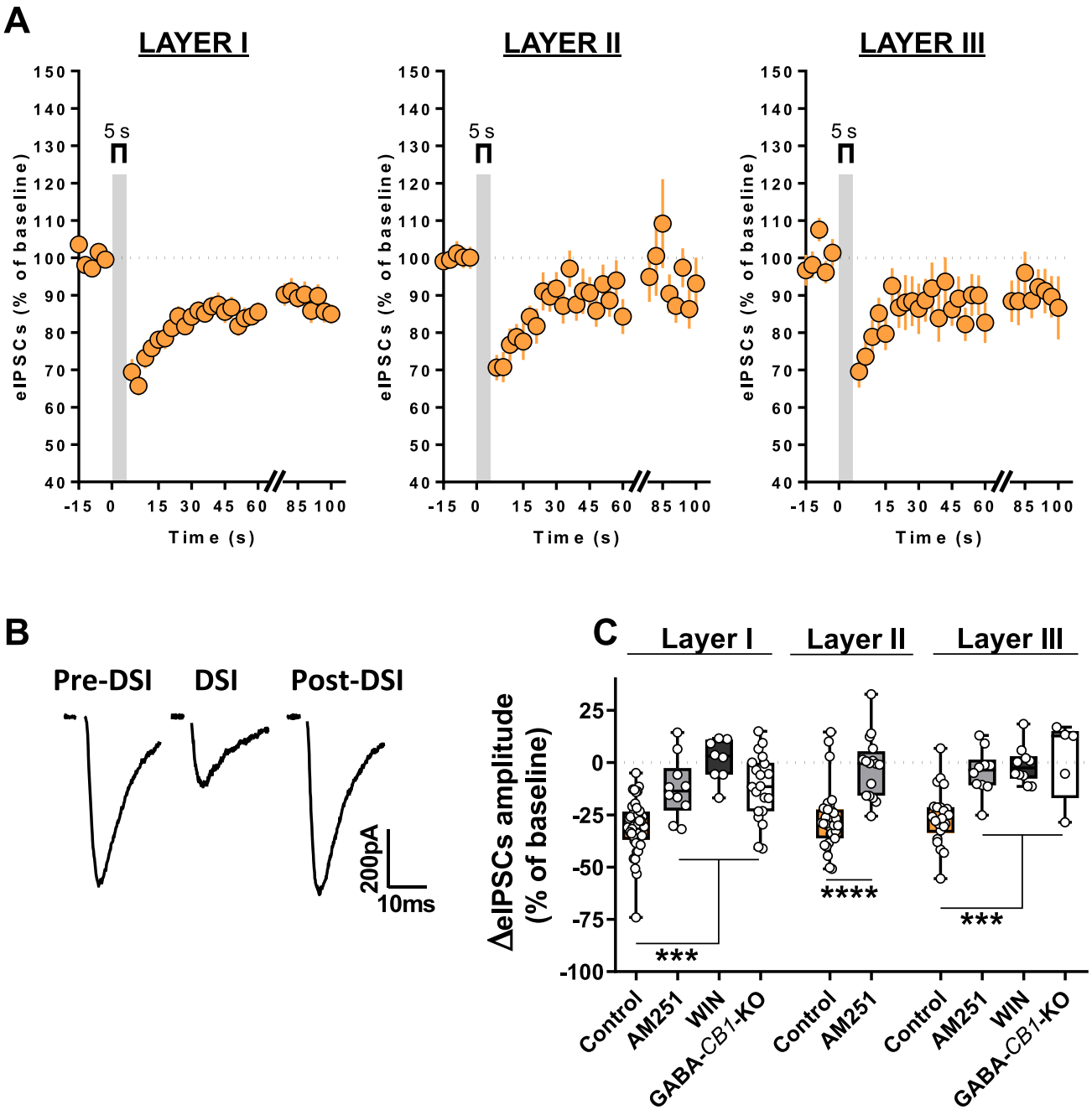

Fig. 2. (A) Temporal effect of 5 s depolarization from −70 mV to 0 mV on eIPSCs obtained in the three layers of wild-type animals. **(B)** Representative traces for a DSI expressed in layer III. Traces were average with the last five sweeps preceding the depolarization (Pre-DSI), the first three sweeps post depolarization (DSI) and five sweeps from 45 to 60 s post depolarization (Post-DSI). **(C)** Percentage of eIPSCs reduction after depolarization. Control (Layer I, $n = 40$; Layer II, $n = 31$ and Layer III, $n = 22$), AM251 (Layer I, $n = 10$; Layer II, $n = 16$ and Layer III, $n = 10$), WIN (Layer I, $n = 8$ and Layer III, $n = 10$), GABA-CB1-KO (Layer I, $n = 20$ and Layer III, $n = 5$). Unpaired *t*-test and one-way ANOVA ($p < 0.0001$), Dunnett post hoc. ****$p < 0.0001$; ***$p < 0.001$. Values are represented mean ± SEM (**A**) and median ± quartiles (**C**). For statistical details, see Table 1.

(0.1 ± 5.3% SEM; Fig. 3B, D) and layer III (3.1 ± 11.7% SEM; Fig. 3C, D), indicating that this form of synaptic plasticity depends on the endogenous activation of CB1 receptors. Thus, ECS-dependent iLTD depends on anatomical constraints, being absent when layer I inhibitory synapses are stimulated.

Layer-dependent neurochemical signatures of CB1-positive interneurons in the aPC

In order to further investigate the reasons of such layer-dependency of aPC iLTD, we next asked whether CB1-positive GABAergic neurons in the different layers display different neurochemical signatures. Based on

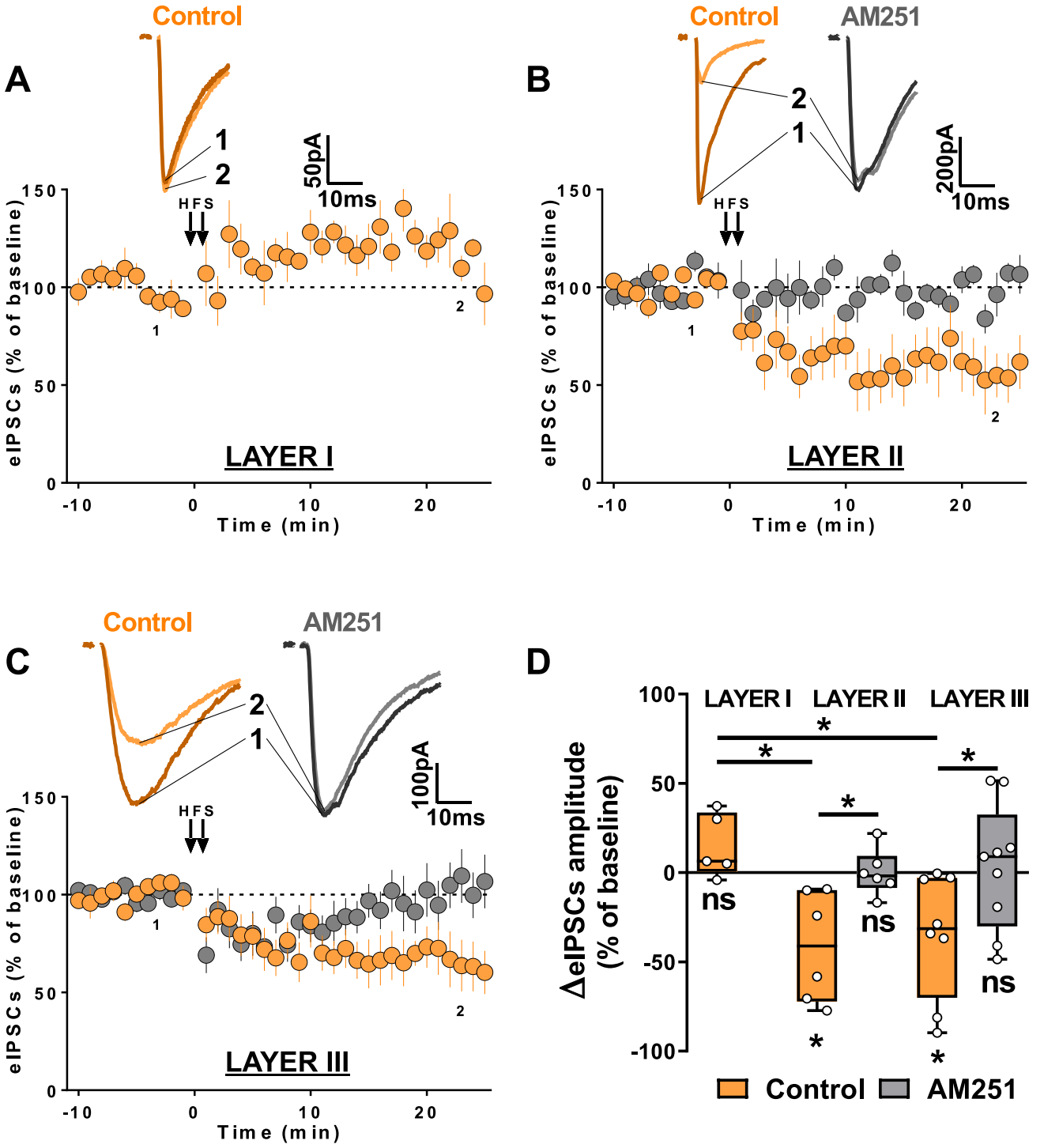

Fig. 3. Effect of HFS on eIPSCs in Layer I **(A)**, Layer II **(B)** and in Layer III **(C)**. Top, representative traces average during the last 5 min before High-Frequency Stimulation (HFS) (1) and 20–25 min after (2). Bottom, eIPSCs time course. **(D)** Average eIPSCs recorded 20–25 min after HFS application normalized to baseline. Layer I (control, $n = 5$), Layer II (control and AM251, $n = 6$), Layer III (control, $n = 8$; AM251, $n = 9$). One-sample *t*-test, unpaired *t*-test and one way-ANOVA ($p < 0.01$), Tukey post hoc. $^*p < 0.05$; ns, not significant. Values are represented mean ± SEM (**A-C**) and median ± quartiles (**D**). For statistical details, see Table 1.

electrophysiological properties, laminar location, morphology and expression of molecular markers, several distinct classes of interneurons have been pointed out in the aPC (Suzuki and Bekkers, 2007, 2010a,b, 2012). Fluorescent *in situ* hybridization (FISH) revealed that, similarly to other brain regions (Marsicano and Lutz, 1999), CB1-positive cells in the aPC contain variable amounts of receptor transcript, ranging from very

high to low-to-moderate levels (Terral et al., 2019). As revealed by double FISH (D-FISH), all high CB1-expressing cells in the aPC are GABAergic interneurons because they co-express mRNAs coding for glutamic acid decarboxylase 65KDa and 67KDa (GAD65/67, 157/157 cells; see methods), whereas cells containing low-to-moderate levels of the CB1 receptor belong only in part to this cellular subpopulation [Fig. 4A; (Terral et al., 2019)]. Moreover, independently of the levels of CB1 receptor transcript, CB1-expressing cells in layer I are virtually all co-expressing GAD65/67 indicating their GABAergic nature [Fig. 4A; (Terral et al., 2019)]. However, in layers II and III, the majority of cells containing low-to-moderate amounts of CB1 mRNA are not GABAergic [Fig. 4A; (Terral et al., 2019)]. In the hippocampus, expression of iLTD characterizes GABAergic interneurons belonging to the family of basket cells containing the neuropeptide cholecystokinin (CCK; Basu et al. 2013; Chevaleyre and Piskorowski 2014). Importantly, anatomical data showed that layer I interneurons in the aPC lack typical markers of GABAergic cells, including CCK (Cummings, 1997; Suzuki and Bekkers, 2007, 2010b). D-FISH experiments with CB1 and CCK mRNA (Fig. 4B) confirmed that, independently of the levels of expression, only 1.7% of CB1-positive neurons in the layer I of the aPC contain CCK mRNA (Fig. 4B, C; 6/359 cells). Consistently, although all high CB1-expressing GABAergic cells do express CCK mRNA, they are abundantly present in layers II and III and are virtually absent from layer I (Fig. 4B, D). Therefore, independently of the levels of expression, the majority of GABAergic CB1-positive interneurons in layer II/III appear to contain CCK, whereas this co-localization is absent in layer I. Thus, CB1-positive GABAergic interneurons in the aPC are characterized by distinct neurochemical signatures that depend on the anatomical layer location.

DISCUSSION

In this study, we characterized the effect of CB1 receptor modulation on inhibitory aPC synapses. We evaluated the impact of exogenous activation of CB1 receptors and the presence of different forms of ECS-dependent synaptic plasticity in relation to the anatomical origin of the inhibitory inputs. We found that anatomical constraints determine the presence and/or properties of CB1 receptor-dependent effects. Moreover, we identified potential neurochemical signatures of local GABAergic interneurons that might be responsible for the expression of long-term forms of CB1 receptor-dependent plasticity of inhibitory synaptic transmission.

WIN-induced decrease of inhibitory transmission and DSI are present when the stimulating electrode is placed in all aPC layers of wild-type mice. Although the amplitude of eIPSCs reached about 90% of baseline values 60–100 s after DSI, the signal did not fully recover. This could be due to specific features of DSI in aPC. However, such lack of complete recovery is also observed in other brain regions (unpublished observations). While the mechanisms involved are not clear, they appear to be linked to the stimulation frequency required to observe DSI, likely inducing synaptic fatigue or habituation processes (Kandel et al., 2012).

Differently from WIN and DSI experiments, iLTD is obtained by stimulating layers II and III inhibitory fibers, whereas the same stimulation protocol does not induce this form of plasticity when applied to layer I. Surprisingly, the intensities and properties of exogenous (WIN) and endogenous effects (iLTD) of CB1 receptor activation appear to be independent of each other. By comparing these effects in the different layers, it appears that the engaged synapses are equally sensitive to exogenous application of WIN in layers I and III, but less in layer II. Conversely, iLTD is equally expressed in layers II and III, but it is absent in layer I. These results suggest that different mechanisms and functions underlie the activity of CB1 receptors at inhibitory synapses in specific aPC layers. For instance, the fact that layer I interneurons respond to WIN (even more strongly than layer II ones) and express DSI, but do not respond to iLTD-inducing stimuli clearly indicate that different machineries are involved in these CB1-dependent effects. Such layer-dependent differences between DSI and iLTD have also been described in the hippocampus, where DSI can be induced both when IPSCs are evoked in *stratum radiatum* and in *stratum pyramidalis*, whereas iLTD occurs only in *stratum radiatum* (Chevaleyre and Castillo, 2003). Frequency of firing and levels of activity of the interneurons have been proposed to play a key role in the modulation of CB1 receptor activity at their synaptic terminals in the hippocampus (Foldy et al., 2006; Heifets et al., 2008; Younts et al., 2016). It will be very interesting to assess if similar phenomena apply to the aPC. Another possibility for iLTD expression could be explained by the presence of high levels of CB1 receptors in interneurons. Considering that layer I contains virtually no high CB1-expressing GABAergic cells, lack of high levels of CB1 receptors in this layer might prevent this form of plasticity.

Our data show that virtually none of the CB1-positive GABAergic interneurons in the layer I of aPC (where WIN has an effect, DSI is present, but no iLTD is observed) express the neuropeptide CCK. This results are surprising as the large majority of GABAergic CB1-positive interneurons throughout the brain are reported to be CCK-positive. However, Marsicano and Lutz (1999) described in the anterior olfactory nucleus that among CB1-positive and CCK-negative neurons, at least 4% are interneurons (containing parvalbumin). Therefore, few, but significant amounts of CCK-negative CB1-positive GABAergic interneurons are likely to exist, especially in olfactory areas. This suggests that, besides the expression of CB1 receptors, neurochemical features of the interneurons might be a key element for iLTD, but not for DSI nor for the pharmacological activation of CB1 receptors in the aPC. Indeed, CCK-positive basket cells have been proposed to be responsible for iLTD in the hippocampus (Basu et al. 2013; Chevaleyre and Piskorowski 2014), possibly explaining why this form of synaptic plasticity in the aPC is restricted to layers II and III, where interneurons expressing both CCK and

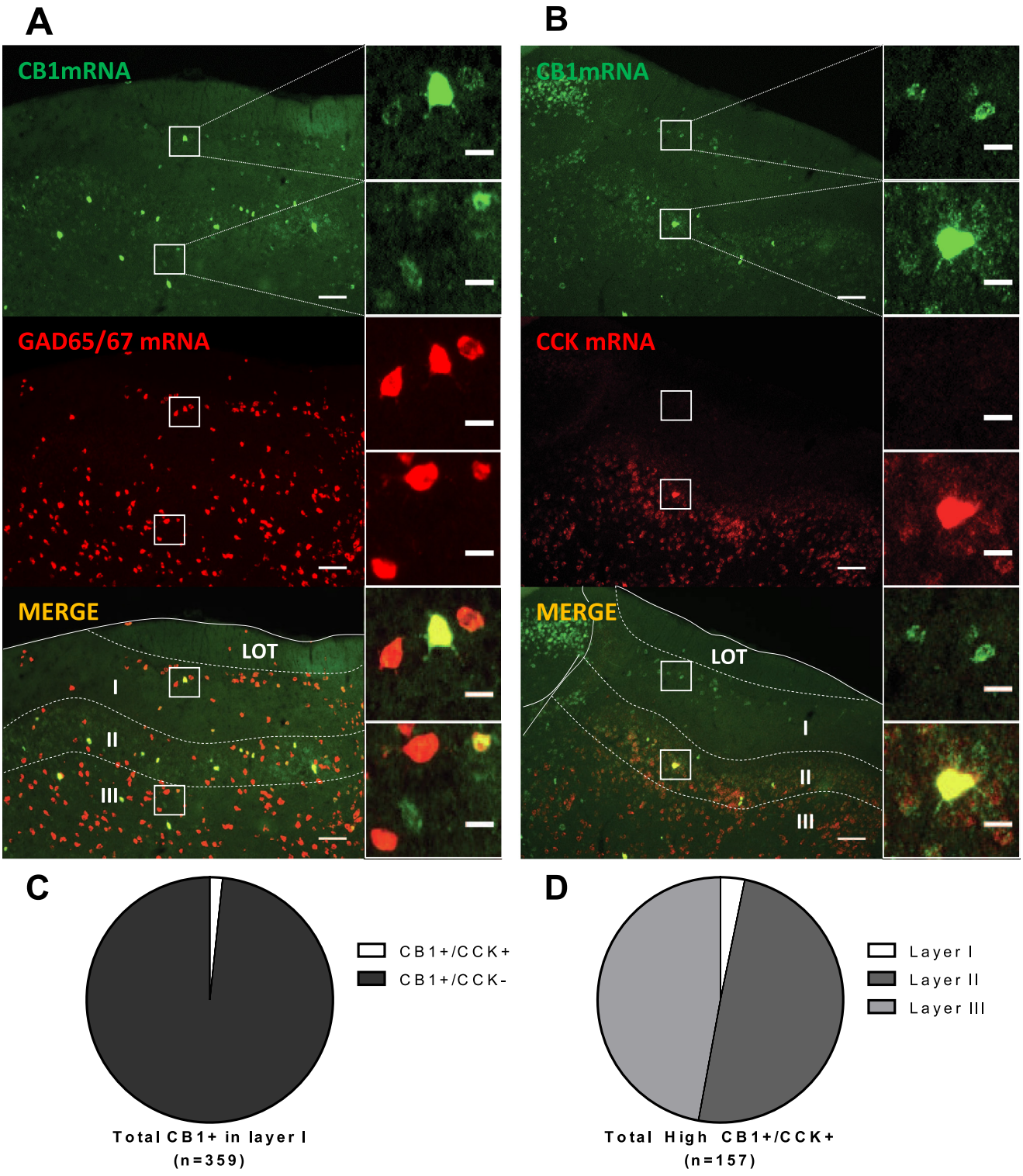

Fig. 4. **(A)** Representatives images of double Fluorescent *In Situ* Hybridization (D-FISH) against CB1mRNA and GAD65/67mRNA or **(B)** with CCK mRNA. **(C)** Distribution of total cells co-localizing CB1 receptor mRNA (CB1+) with CCK mRNA (CCK+) in layer I (CB1+/CCK+, 1.7%). Scale bar, 100 μm; scale bar inserts, 20 μm. **(D)** Distribution of cells co-expressing high CB1-levels with CCK marker (Layer I, 3.2%; Layer II, 49.7%; Layer III, 47.1%).

CB1 are abundantly present. Thus, together with the results obtained in the hippocampus, our data strengthen the idea that a sort of CCK-dependency exists for iLTD but not for DSI or for exogenous cannabinoid agonist effects. As in other brain regions (Marsicano and Lutz, 1999), CCK is present in both GABAergic and glutamatergic neurons of aPC layers II and III (Cummings, 1997; Fig. 4), making the specific targeting of GABAergic-

CCK-positive cells very challenging (Dimidschstein et al., 2016; Busquets-Garcia et al., 2018b). Thus, one can speculate that the presence of CCK in interneurons might functionally participate in iLTD induction in the aPC. Future technological advances such as intersectional strategies (Taniguchi et al., 2011) will hopefully help addressing these interesting questions.

Besides specific neurochemical features of the interneurons, several other hypotheses might explain the lack of iLTD in layer I. For instance, intrinsic molecular mechanisms could explain the different layer sensitivity of interneurons to CB1 receptor-dependent forms of synaptic plasticity. For instance, Younts et al., (2016) demonstrated that iLTD induction (but not DSI) requires pre-synaptic protein synthesis. Thus, it could be possible that the machinery necessary for the expression or the activation of protein synthesis might differ between layer I and layer II/III inhibitory inputs. Moreover, most forms of iLTD have been shown to depend on the activation of metabotropic glutamate receptors (mGluRs) in different brain regions (Kano et al., 2009). Thus, the iLTD layer-dependence could result from the presence or not of these postsynaptic receptors. However, data indicate that stimulation of layer I fibers evokes postsynaptic mGluR receptor-dependent effects in aPC principal neurons (Sugitani et al., 2002, 2004), suggesting that the lack of iLTD in this location is unlikely to be ascribed to lack of recruitment of metabotropic glutamate signaling. Specific anatomical constraints might also explain the lack of layer I iLTD. Data from Suzuki and Bekkers (2010a) suggest that, differently from layers II and III, layer I aPC interneurons do not seem to form perisomatic terminals around principal cells. Therefore, the stimulation of perisomatic innervation might represent a required feature for iLTD in the aPC. It is however possible that stimulation in layer I might activate collaterals of perisomatic basket cells located in layer II. In this case, the lack of layer I iLTD might be due to the physical distance of layer I excitatory synapses potentially undergoing glutamatergic spillover from iLTD-prone GABAergic synapses (Castillo et al., 2012). Future studies will address the detailed mechanisms underlying the layer-dependent expression of iLTD in the aPC.

In conclusion, this study shows that, inhibitory synapses in the aPC are under a layer-dependent differential control by CB1 receptors. These data suggest that CB1 receptors play an important role in the selective control of excitatory/inhibitory balance potentially regulating brain odor responses. As the retrieval of appetitive olfactory memory has been recently associated with a general CB1 receptor-dependent control of inhibitory transmission (Terral et al., 2019), these data indicate that layer-specific DSI and/or iLTD in the aPC might directly participate in the regulation of olfactory-dependent behaviors.

ACKNOWLEDGMENTS

We thank all the personal of the Animal Facility of the NeuroCentre Magendie for mouse care and genotyping. We also thank Gabriel Lepousez, Antoine Nissant, Pierre-Marie Lledo, Wilfrid Mazier and all the members of Marsicano's lab for useful discussions. This work was supported by INSERM (to G.M.), INRAE (to G.F.), Fondation pour la Recherche Médicale (DRM 20101220445 to G.M. and FDT20170436845 to G.T.), French State/Agence Nationale de la Recherche (LABEX BRAIN ANR-10-LABX-43 to G.M., G.F, NeuroNutriSens ANR-13-BSV4-0006-02 to G.M., Orups ANR-16-CE37-0010 to G.M. and G.F., CaCoVi ANR-18-CE16-0001 to G.M., MitObesity ANR-18-CE14-0029 to G.M.), EU-FP7 (PAINCAGE, HEALTH-603191 to G.M., European Research Council (Endofood, ERC-2010-StG-260515, CannaPreg, ERC-2014-PoC-640923 and MiCaBra, ERC-2017-AdG-786467, to G.M.), Human Frontiers Science Program (to G.M.), Region Aquitaine (to G.M.).

CONFLICT OF INTEREST STATEMENT

The authors declare no competing interests.

AUTHOR CONTRIBUTIONS

G.T., G.F., and G.M. designed research; G.T., M.J., A.C. performed research; G.T., F.M., G.F. and G.M. supervised research; G.T. analyzed data; G.T., G.F., and G.M. wrote the manuscript. All authors edited and approved the manuscript.

REFERENCES

Araque A, Castillo PE, Manzoni OJ, Tonini R (2017) Synaptic functions of endocannabinoid signaling in health and disease. Neuropharmacology 124:13–24.

Avery MC, Krichmar JL (2017) Neuromodulatory systems and their interactions: a review of models, theories, and experiments. Front Neural Circuits 11.

Basu J, Srinivas KV, Cheung SK, Taniguchi H, Huang ZJ, Siegelbaum SA (2013) A cortico-hippocampal learning rule shapes inhibitory microcircuit activity to enhance hippocampal information flow. Neuron 79:1208–1221.

Bellocchio L, Lafenêtre P, Cannich A, Cota D, Puente N, Grandes P, Chaouloff F, Piazza PV, Marsicano G (2010) Bimodal control of stimulated food intake by the endocannabinoid system. Nat Neurosci 13:281–283.

Bénard G, Massa F, Puente N, Lourenço J, Bellocchio L, Soria-Gómez E, Matias I, Delamarre A, Metna-Laurent M, Cannich A, et al. (2012) Mitochondrial CB1 receptors regulate neuronal energy metabolism. Nat Neurosci 15:558–564.

Betke KM, Wells CA, Hamm HE (2012) GPCR mediated regulation of synaptic transmission. Prog Neurobiol 96:304–321.

Bolding KA, Franks KM (2018) Recurrent cortical circuits implement concentration-invariant odor coding. Science.

Busquets-Garcia, Bains J, Marsicano G (2018a) CB1 receptor signaling in the brain: extracting specificity from ubiquity. Neuropsychopharmacology 43:4–20.

Busquets-Garcia, Oliveira da Cruz JF, Terral G, Zottola ACP, Soria-Gómez E, Contini A, Martin H, Redon B, Varilh M, Ioannidou C, et al. (2018b) Hippocampal CB1 receptors control incidental associations. Neuron 99:1247–1259.

Castillo PE, Younts TJ, Chávez AE, Hashimotodani Y (2012) Endocannabinoid signaling and synaptic function. Neuron 76:70–81.

Chevaleyre V, Castillo PE (2003) Heterosynaptic LTD of hippocampal GABAergic synapses: a novel role of endocannabinoids in regulating excitability. Neuron 38:461–472.

Chevaleyre V, Castillo PE (2004) Endocannabinoid-mediated metaplasticity in the hippocampus. Neuron 43:871–881.

Chevaleyre V, Piskorowski R (2014) Modulating excitation through plasticity at inhibitory synapses. Front Cell Neurosci 8.
Crosby KM, Inoue W, Pittman QJ, Bains JS (2011) Endocannabinoids gate state-dependent plasticity of synaptic inhibition in feeding circuits. Neuron 71:529–541.
Cummings SL (1997) Neuropeptide Y, somatostatin, and cholecystokinin of the anterior piriform cortex. Cell Tissue Res 289:39–51.
Dimidschstein J, Chen Q, Tremblay R, Rogers SL, Saldi G-A, Guo L, Xu Q, Liu R, Lu C, Chu J, et al. (2016) A viral strategy for targeting and manipulating interneurons across vertebrate species. Nat Neurosci 19:1743–1749.
Foldy C, Neu A, Jones MV, Soltesz I (2006) Presynaptic, activity-dependent modulation of cannabinoid type 1 receptor-mediated inhibition of GABA release. J Neurosci 26:1465–1469.
Franks KM, Russo MJ, Sosulski DL, Mulligan AA, Siegelbaum SA, Axel R (2011) Recurrent circuitry dynamically shapes the activation of piriform cortex. Neuron 72:49–56.
Heifets BD, Chevaleyre V, Castillo PE (2008) Interneuron activity controls endocannabinoid-mediated presynaptic plasticity through calcineurin. Proc Natl Acad Sci 105:10250–10255.
Herkenham M, Lynn AB, Little MD, Johnson MR, Melvin LS, de Costa BR, Rice KC (1990) Cannabinoid receptor localization in brain. Proc Natl Acad Sci 87:1932–1936.
Howlett AC, Barth F, Bonner TI, Cabral G, Casellas P, Devane A, Felder CC, Herkenham M, Mackie K, Martin BR, et al. (2002) International union of pharmacology. XXVII. Classification of cannabinoid receptors. Pharmacol Rev 54:161–202.
Huang Y, Thathiah A (2015) Regulation of neuronal communication by G protein-coupled receptors. FEBS Lett 589:1607–1619.
Kandel ER, Schwartz JH, Jessel TM, Siegelbaum SA, Hudspeth AJ (2012). Principles of neural science. 5th ed.
Kano M, Ohno-Shosaku T, Hashimotodani Y, Uchigashima M, Watanabe M (2009) Endocannabinoid-mediated control of synaptic transmission. Physiol Rev 89:309–380.
Marsicano G, Kuner R (2008) Anatomical distribution of receptors, ligands and enzymes in the brain and in the spinal cord: circuitries and neurochemistry. In: Köfalvi A, editor. Cannabinoids and the brain. Boston, MA: Springer US. p. 161–201.
Marsicano G, Goodenough S, Monory K, Hermann H, Eder M, Cannich A, Azad SC, Cascio MG, Gutiérrez SO, van der Stelt M, et al. (2003) CB1 cannabinoid receptors and on-demand defense against excitotoxicity. Science 302:84–88.
Marsicano, Lutz B (1999) Expression of the cannabinoid receptor CB1 in distinct neuronal subpopulations in the adult mouse forebrain. Eur J Neurosci 11:4213–4225.
Marsicano G, Wotjak CT, Azad SC, Bisogno T, Rammes G, Cascio MG, Hermann H, Tang J, Hofmann C, Zieglgänsberger W, et al. (2002) The endogenous cannabinoid system controls extinction of aversive memories. Nature 418:530–534.
Monory, Massa F, Egertová M, Eder M, Blaudzun H, Westenbroek R, Kelsch W, Jacob W, Marsch R, Ekker M, et al. (2006) The endocannabinoid system controls key epileptogenic circuits in the hippocampus. Neuron 51:455–466.
Nadim F, Bucher D (2014) Neuromodulation of neurons and synapses. Curr Opin Neurobiol 29:48–56.
Piazza PV, Cota D, Marsicano G (2017) The CB1 receptor as the cornerstone of exostasis. Neuron 93:1252–1274.
Piomelli D (2003) The molecular logic of endocannabinoid signalling. Nat Rev Neurosci 4:873–884.
Poo C, Isaacson JS (2009) Odor representations in olfactory cortex: "sparse" coding, global inhibition, and oscillations. Neuron 62:850–861.
Pouille F, Schoppa NE (2018) Cannabinoid receptors modulate excitation of an olfactory bulb local circuit by cortical feedback. Front Cell Neurosci 12.
Soria-Gómez E, Bellocchio L, Reguero L, Lepousez G, Martin C, Bendahmane M, Ruehle S, Remmers F, Desprez T, Matias I, et al. (2014) The endocannabinoid system controls food intake via olfactory processes. Nat Neurosci 17:407–415.
Sugitani M, Sugai T, Onoda N (2002) Postsynaptic activity of metabotropic glutamate receptors in the piriform cortex. Neuroreport 13:1473–1476.
Sugitani M, Sugai T, Onoda N (2004) Postsynaptic metabotropic glutamate receptor mGluR1 mediates the late component of signal propagation in the guinea pig piriform cortex: optical imaging study. Neurosci Lett 356:29–32.
Suzuki, Bekkers JM (2006) Neural coding by two classes of principal cells in the mouse piriform. Cortex J. Neurosci 26:11938–11947.
Suzuki, Bekkers JM (2007) Inhibitory interneurons in the piriform cortex. Clin Exp Pharmacol Physiol 34:1064–1069.
Suzuki, Bekkers JM (2010b) Inhibitory neurons in the anterior piriform cortex of the mouse: classification using molecular markers. J Comp Neurol 518:1670–1687.
Suzuki, Bekkers JM (2010a) Distinctive classes of GABAergic interneurons provide layer-specific phasic inhibition in the anterior piriform cortex. Cereb Cortex 20:2971–2984.
Suzuki N, Bekkers JM (2011) Two layers of synaptic processing by principal neurons in piriform cortex. J Neurosci 31:2156–2166.
Suzuki, Bekkers JM (2012) Microcircuits mediating feedforward and feedback synaptic inhibition in the piriform cortex. J Neurosci 32:919–931.
Taniguchi H, He M, Wu P, Kim S, Paik R, Sugino K, Kvitsani D, Fu Y, Lu J, Lin Y, et al. (2011) A resource of Cre driver lines for genetic targeting of GABAergic neurons in cerebral cortex. Neuron 71:995–1013.
Terral G, Busquets-Garcia A, Varilh M, Achicallende S, Cannich A, Bellocchio L, Bonilla-Del Río I, Massa F, Puente N, Soria-Gomez E, et al. (2019) CB1 receptors in the anterior piriform cortex control odor preference memory. Curr. Biol. 29:2455–2464.
Wang Z-J, Sun L, Heinbockel T (2012) Cannabinoid receptor-mediated regulation of neuronal activity and signaling in glomeruli of the main olfactory bulb. J Neurosci 32:8475–8479.
Wang Z-J, Hu SS-J, Bradshaw HB, Sun L, Mackie K, Straiker A, Heinbockel T (2019) Cannabinoid receptor-mediated modulation of inhibitory inputs to mitral cells in the main olfactory bulb. J Neurophysiol.
Wilson R.A. Nicoll Endogenous cannabinoids mediate retrograde signalling at hippocampal synapses Nature 410 2001 588 592
Younts, Monday HR, Dudok B, Klein ME, Jordan BA, Katona I, Castillo PE (2016) Presynaptic protein synthesis is required for long-term plasticity of GABA release. Neuron 92:479–492.
Zhan C, Luo M (2010) Diverse patterns of odor representation by neurons in the anterior piriform cortex of awake mice. J Neurosci 30:16662–16672.
Zou S, Kumar U (2018) Cannabinoid receptors and the endocannabinoid system: signaling and function in the central nervous system. Int. J. Mol Sci 19.

(Received 5 November 2019, Accepted 3 March 2020)
(Available online 12 March 2020)